Tohoku J. Exp. Med., 2018, **246**, 1-8

Demonstration of Mitochondrial Damage and Mitophagy in Cisplatin-Mediated Nephrotoxicity

Miki Ichinomiya,[1,*] Akinori Shimada,[1] Naoki Ohta,[1,*] Erina Inouchi,[1] Kikumi Ogihara,[1] Yuko Naya,[1] Masaki Nagane,[2] Takehito Morita[3] and Masahiko Satoh[4]

[1]Laboratory of Pathology, School of Life and Environmental Science, Azabu University, Sagamihara, Kanagawa, Japan
[2]Laboratory of Biochemistry, School of Veterinary Medicine, Azabu University, Sagamihara, Kanagawa, Japan
[3]Department of Veterinary Pathology, Tottori University, Tottori, Tottori, Japan
[4]Laboratory of Pharmaceutical Health Sciences, School of Pharmacy, Aichi Gakuin University, Nagoya, Aichi, Japan

Cisplatin is a chemotherapeutic widely used in the treatment of various types of solid tumors. Acute kidney injury is the most critical dose-limiting factor in cancer patients treated with cisplatin; mitochondrial dysfunction and resultant cell damage by reactive oxygen species released from damaged mitochondria are suspected to be involved in the kidney injury. Pathological features of mitochondrial damage in relation to cisplatin-mediated nephrotoxicity, however, is not fully described. The purpose of this study was to demonstrate mitochondrial damage and clearance of damaged mitochondria by mitophagy in cisplatin-mediated nephrotoxicity. Three groups of rats received a single intraperitoneal injection of cisplatin at 20 mg/kg and were sacrificed at 24, 48 and 72 hours after the treatment. A time-dependent increase in the number of damaged renal tubules and the serum levels of blood urea nitrogen, creatinine, and mitochondrial aspartate transaminase was observed in rats after the treatment. We showed the increased numbers of swollen and fragmented mitochondria, observed by electron microscopy, and of cytochrome c oxidase IV- and 8-nitroguanosine-positive intracytoplasmic granules, detected by immunohistochemistry, in the degenerated renal tubules of the treated animals. Moreover, activated autophagy process was indicated in the degenerated renal epithelial cells, based on the findings of immunohistochemistry of microtubule-associated protein 1 light chain 3 (LC3), an autophagy marker, and lysosomal-associated membrane protein 1 (LAMP-1), a lysosome marker, and swollen and fragmented mitochondria in autophagosomes. These results suggest that mitochondrial damage and clearance of damaged mitochondria by mitophagy is involved in cisplatin-mediated nephrotoxicity.

Keywords: cisplatin; mitochondria; mitophagy; nephrotoxicity; rat
Tohoku J. Exp. Med., 2018 September, **246** (1), 1-8.

Introduction

Nephrotoxicity is a major side effect of cisplatin in chemotherapy (Sastry and Kellie 2005; Tsang et al. 2009). Pathologically, cisplatin-mediated nephrotoxicity is characterized by cell damage and death in renal tubules. Although the exact mechanism underlying cisplatin-mediated nephrotoxicity is not clear, it has been suggested that cisplatin, accumulated in mitochondria, causes mitochondrial dysfunction, ultimately resulting in proximal tubular cells death caused by reactive oxygen species (ROS) released from damaged mitochondria (Choi et al. 2015). Autophagy is the process responsible for recycling organelles and long-lived proteins to maintain cellular homeostasis (He and Klionsky 2009). Targeted degradation of mitochondria by the autophagic machinery is referred to as mitophagy. Based on the results of the experiment with the use of autophagy-deficient mice, previous studies indicated that in cisplatin-mediated nephrotoxicity, autophagy eliminates ROS-producing damaged mitochondria, presumably through mitophagy (Periyasamy-Thandavan et al. 2008; Takahashi et al. 2012). However, the detailed pathological process of cisplatin-mediated nephrotoxicity, with special emphasis on the mitochondrial damage and subsequent mitophagy, has not been fully described. The purpose of this study was to demonstrate the pathological features

Received June 18, 2018; revised and accepted August 13, 2018. Published online September 1, 2018; doi: 10.1620/tjem.246.1.
*These authors contributed equally to this work.
Correspondince: Akinori Shimada, Laboratory of Pathology, School of Life and Environmental Science, Azabu University, 1-17-71 Fuchinobe, Chuo-ku, Sagamihara, Kanagawa 252-5201, Japan.
e-mail: a-shimada@azabu-u.ac.jp

of mitochondrial damage and clearance of damaged mitochondria by mitophagy in cisplatin-mediated nephrotoxicity.

Materials and Methods

Animals and drug treatments

A total of 20 male Wistar rat, 6 weeks old, were obtained from CLEA JAPAN Inc. (Tokyo, Japan). The rats were housed in cages at a temperature of approximately 25˚C with 55-70% humidity. All the experiments were performed according to the guidelines of The Laboratory Animal Care Committee of Azabu University. Rats were divided into a control group (n = 5) and three treatment groups (n = 5) divided as follows: 24-hour group, 48-hour group and 72-hour group. The rats in the three treatment groups received a single intraperitoneal injection of cisplatin, dissolved in saline solution, at a dose of 20 mg/kg (cisdiammineplatinum (II) dichloride; Wako, Osaka, Japan) and were sacrificed at 24, 48, and 72 hours after the treatment, respectively. Control group of rats received a single intraperitoneal injection of vehicle (saline solution).

Serum biochemistry analysis

Serum levels of creatinine, blood urea nitrogen (BUN), and total (t)-aspartate transaminase (AST), were measured using a 7180 Clinical Analyzer (Hitachi, Tokyo, Japan). Mitochondrial (m)-AST was measured using JCA-BM 8000 Clinical Chemistry Analyzer (JEOL, Tokyo, Japan).

Histological examination

Following fixation of the kidneys with 10% formalin, renal tissues were sectioned and stained with hematoxylin and eosin (HE) for histological examination. Tubular damage in HE-stained sections was examined under the microscope and scored based on the number of degenerated tubules and degree of degeneration. A semiquantitative evaluation of the tubular damage was conducted by calculation of the counted number of degenerated tubules in ten randomly chosen microscopic fields at × 400 and degree of degeneration of tubules: tubular degeneration was graded subjectively on a scale of 1, 3 and 5 (1 = very mild degeneration, tubules consisting of epithelial cells showing a few small cytoplasmic vacuoles; 3 = moderate degeneration, tubules consisting of epithelial cells showing larger number of cytoplasmic vacuoles of variable size; and 5 = very severe degeneration, tubules showing necrosis and loss of epithelial cells). These measurements were performed five times and the mean values were calculated and recorded.

Western blot analysis

The frozen kidney tissues were lysed with a RIPA lysis buffer (50 mM Tris-Cl [pH 7.6], 150 mM NaCl, 1% NP-40, 0.1% SDS, 0.5% deoxycholic acid, 1 μg/ml leupeptin, 1 μg/ml aprotinin, and 0.5 mM phenylmethylsulfonyl fluoride) and were centrifuged at 12,000 g at 4°C for 30 minutes to obtain the cellular proteins in the supernatant. Equal amounts of proteins from each sample were resolved by SDS-PAGE, transferred to NC membranes, blocked with 5% skimmed milk for 1 hour at 25°C, and probed at 4°C overnight with the following primary antibodies: rabbit anti-α-tubulin polyclonal antibody (bs-50500R, BIS, MA, USA) at 1:2,000, rabbit anti-cytochrome c oxidase (COX) IV polyclonal antibody (GTX114330, GNT, CA, USA) at 1:1,000, and rabbit polyclonal antibody (bs-8878R, BIS) against human microtubule-associated protein 1 light chain 3 (LC3), an autophagy marker, at 1:1,000. Blots were subsequently probed with horseradish peroxidase-conjugated anti-rabbit IgG (Dako, Glostrup, Denmark) at 1:1,000-5,000. Immunoreactive bands were visualized by enhanced chemiluminescence. The intensity of the bands was analyzed with computer ImageJ software (http://imagej.nih.gov/ij/).

Immunohistochemistry: polymer method

Paraffin-embedded sections of kidney tissues were used for the immunohistochemical detection of COX IV, 8-nitroguanosine, LC-3, and lysosomal-associated membrane protein 1 (LAMP-1). Serial sections were used to identify the location of the two sets of positive reactions in the cytoplasm of the renal epithelial cells: COX IV and 8-nitroguanosine, LC-3, and LAMP-1. For antigen retrieval, the sections were placed in a citrate buffer solution (pH 5.4) and microwaved for 20 min. Endogenous peroxidase activity was quenched with 3% H_2O_2 for 30 min at 25˚C. The slides were then blocked using 10% goat serum in PBS for 1 hour at 25˚C. Thereafter, sections were incubated with the primary antibodies overnight at 4˚C: anti-COX IV, 1:200 dilution; anti-8-nitroguanosine (KMU-P01, CAC, Tokyo, Japan), 1:200 dilution; anti-LC-3, 1:400 dilution; anti-LAMP-1 (bs-1970R, BIS), 1:400 dilution). The primary antibodies were replaced with phosphate-buffered saline (PBS) in negative controls. After incubation with primary antibodies, the sections were placed in a solution containing a peroxidase-labeled polymer conjugated to a secondary anti-rabbit antibody [EnVision + kit / HRP (DAB), Dako, Glostrup] for 30 min at 25˚C. Positive regions were stained in brown with the chromogen 3,3′-diaminobenzidine tetrahydrochloride (DAB) (Wako). Following this process, sections were counterstained with hematoxylin. A semiquantitative evaluation of the immunohistochemical reactions (8-nitroguanosine, LC-3) was conducted by counting the number of stained cells in 10 microscopic fields at × 400 magnification. This step was performed five times and the mean values were calculated and recorded.

Statistical analysis

Statistical analysis of semiquantitative histology and immunohistochemistry was performed using a Student's *t*-test for two-group comparison. For all comparisons, *p* values less than 1% ($p < 0.01$) and 5% ($p < 0.05$) were considered statistically significant.

Transmission electron microscopy

Cubes of 1-2 mm^3 were prepared from kidney tissue. They were fixed in 2.5% glutaraldehyde for 3 hours at 4˚C, rinsed in 0.1 M phosphate buffer (pH = 7.4), post fixed for 1 hour in 1% osmium tetroxide, dehydrated in alcohol, and embedded in epoxy resin. Semithin (1 μm) sections were stained using 1% toluidine blue for electron microscopy examination. Ultra-thin sections stained with uranyl acetate and lead citrate were then examined under a Hitachi H-500H electron microscope (Tokyo, Japan).

Results

To examine the pathological features of mitochondrial damage in cisplatin-mediated nephrotoxicity, three groups of rats were treated with cisplatin and were sacrificed at 24, 48 and 72 hours after the treatment. When samples were examined, results showed that BUN and serum creatinine levels were significantly higher than control values in 48-

and 72-hour groups (Fig. 1). Total-AST and m-AST levels appeared to increase over time; however, a statistical significance was not observed (Fig. 1). Gross pathology demonstrated pale discoloration of the renal cortex; the change was prominent at 72 hours after treatment (Fig. 2). Tubular damage, characterized by epithelial cell necrosis, vacuolar

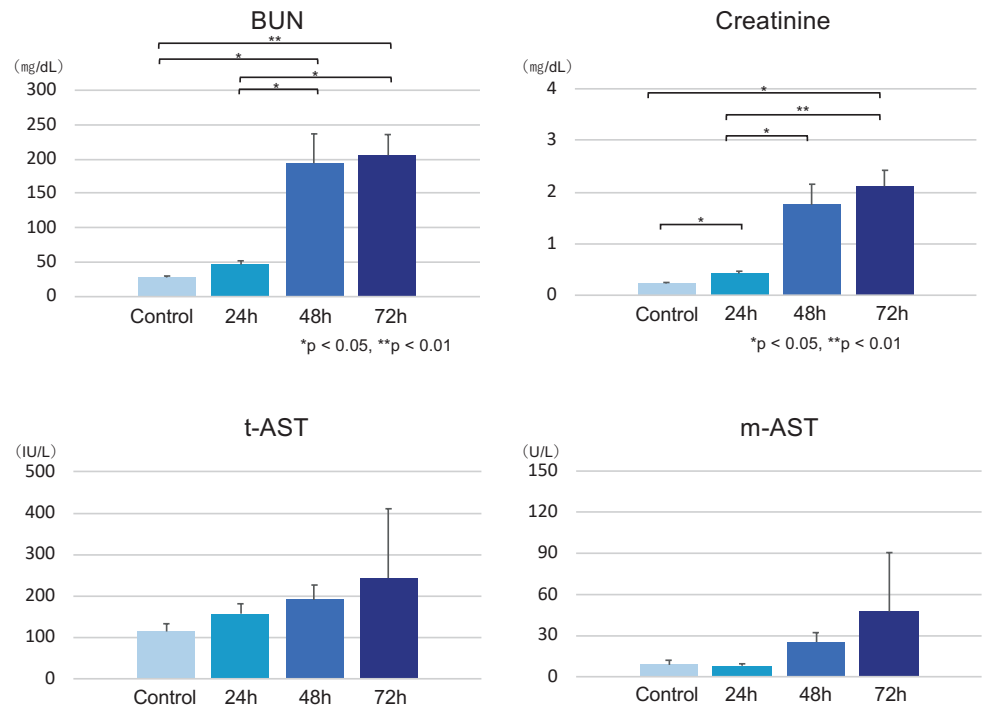

Fig. 1. Serum biochemistry analysis of BUN, creatinine, t-AST, m-AST in rats treated with cisplatin.
BUN, blood urea nitrogen; t-AST, total-aspartate transaminase; m-AST, mitochondrial-aspartate transaminase; h, hour.
All data are expressed as mean ± SD. Statistically significant differences (*p < 0.05, **p < 0.01) are indicated.

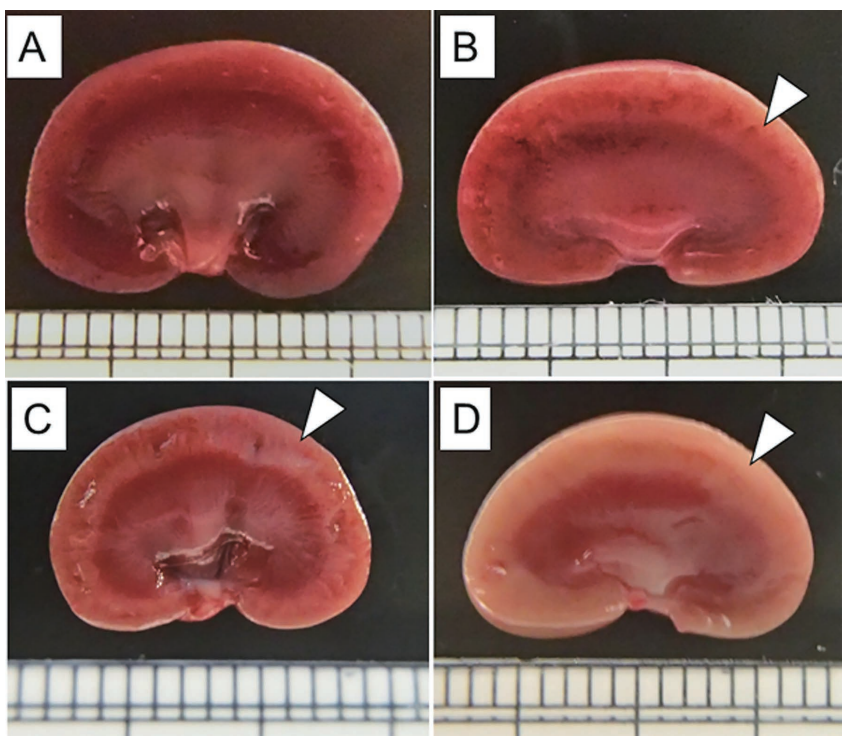

Fig. 2. Gross findings of the kidneys obtained from cisplatin-treated rats.
Pale discoloration (white arrow heads) of the renal cortex is shown in the treated kidneys. The change is prominent in D.
A, control; B, 24 hours after cisplatin treatment; C, 48 hours after cisplatin treatment; D, 72 hours after cisplatin treatment.

degeneration, and regeneration of the proximal convoluted tubules were observed (Fig. 3a). Renal histopathological scoring indicated significant time-dependent renal injury compared to controls (Fig. 3b).

The increase in the number of COX IV-positive granules was observed in the cytoplasm of the renal epithelial cells in treated kidneys; larger granules were extensively accumulated in the degenerated tubules of kidneys treated for 72 hours (Fig. 4a). Western blot analysis of COX IV protein demonstrated the increase at 24 and 48 hours followed by the decrease at 72 hours after treatment (Fig. 4c).

Oxidative stress caused by ROS may damage macromolecules, including DNA, proteins, and lipids, and subcellular organelles, including mitochondria. To characterize the cisplatin-induced DNA damage in renal tissues, immunohistochemistry was conducted to localize 8-nitroguanosine, an oxidized byproduct of nuclear and mitochondrial DNA. In treated kidneys, a positive 8-nitroguanosine staining was present in both nucleus and cytoplasm of the epithelial cells (Fig. 4a); positive immunolabeling in the cytoplasm was interpreted as mitochondrial DNA damage. Moreover, the intensity of the immunostaining was consistently and significantly increased in 48- and 72-hour treated kidneys compared with control kidneys (Fig. 4b). Serial sections of the renal tissue demonstrated co-localization of the immunopositive granules of COX IV and 8-nitroguanosine (Fig. 4a).

Increase in the number of both LC-3- and LAMP-1-positive granules was also observed in the cytoplasm of the renal epithelial cells; granules were present extensively in the degenerated tubules in 72-hour treated kidneys (Fig. 5a, b). The analysis of serial sections of renal tissues showed co-localization of the LC-3 and LAMP-1 immunostainings in granules, indicating an active autophagy process (Fig. 5a). An increase in LC-3 positivity was shown by western blot analysis (Fig. 5c).

Electron microscopy showed an increase of swollen and fragmented mitochondria; some of which were observed in autophagosomes (Fig. 6), indicating clearance of damaged mitochondria by mitophagy.

Discussion

Cisplatin-induced kidney injury has been previously described in mouse models, where focal loss of brush borders, tubular cell vacuolization, tubular dilation, nuclear pyknosis, and cell death were observed in the proximal tubules three days after cisplatin administration (Dobyan et al. 1980; Racusen and Solez 1986; Mukhopadhyay et al. 2012; Zsengellér et al. 2012). These findings are consistent with our present study conducted in a rat model. In our

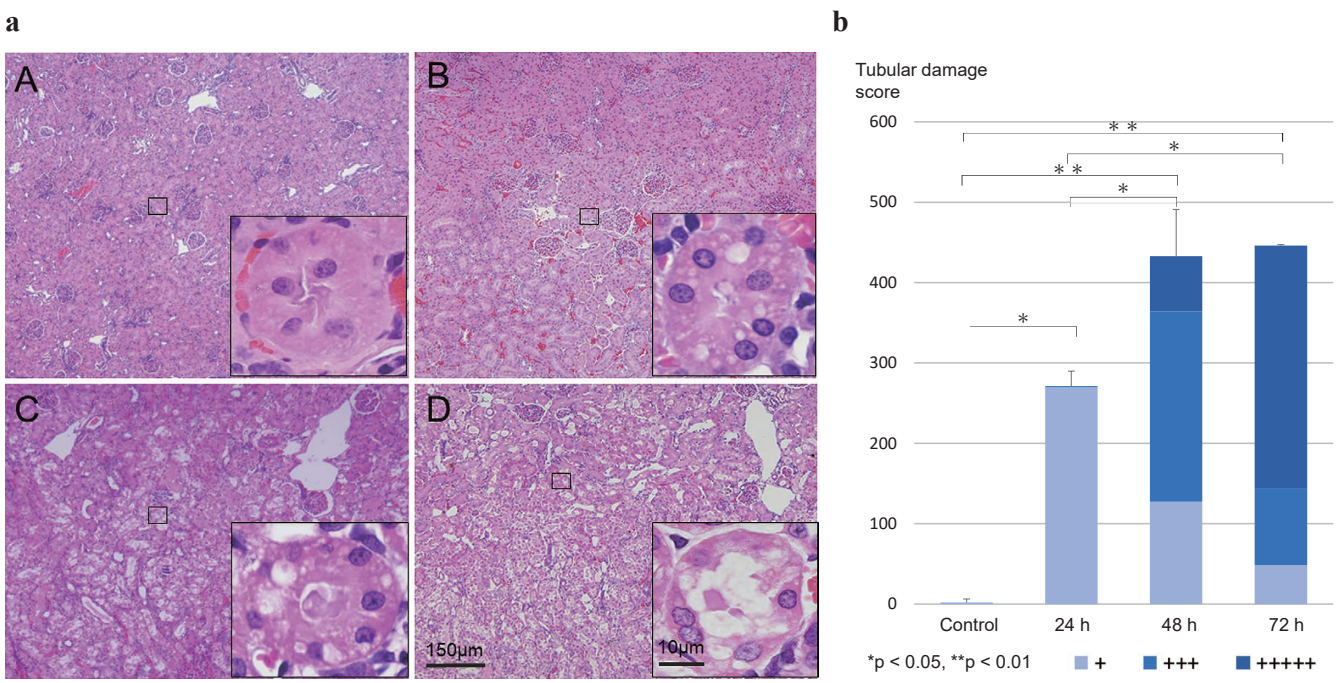

Fig. 3. Light microscopy of the kidney tissues obtained from cisplatin-treated rats.
a. Microscopic findings of the kidney tissues stained with hematoxylin and eosin. Tubular damage, characterized by vacuolar degeneration and necrosis of the epithelial cells, is observed in the treated kidneys. Larger area of the tubular degeneration is shown in D. Inset: higher power magnification of the affected cortex (rectangle), showing severe vacuolar changes and loss of the renal epithelial cells in D.
A, control; B, 24 hours after cisplatin treatment; C, 48 hours after cisplatin treatment; D, 72 hours after cisplatin treatment.
b. Renal histopathological scoring. Time-dependent increase in the renal injury is shown.
h, hour; +, mild degeneration; +++, moderate degeneration; +++++, very severe degeneration.
All data are expressed as mean ± SD. Statistically significant differences (*p < 0.05, **p < 0.01) are indicated.

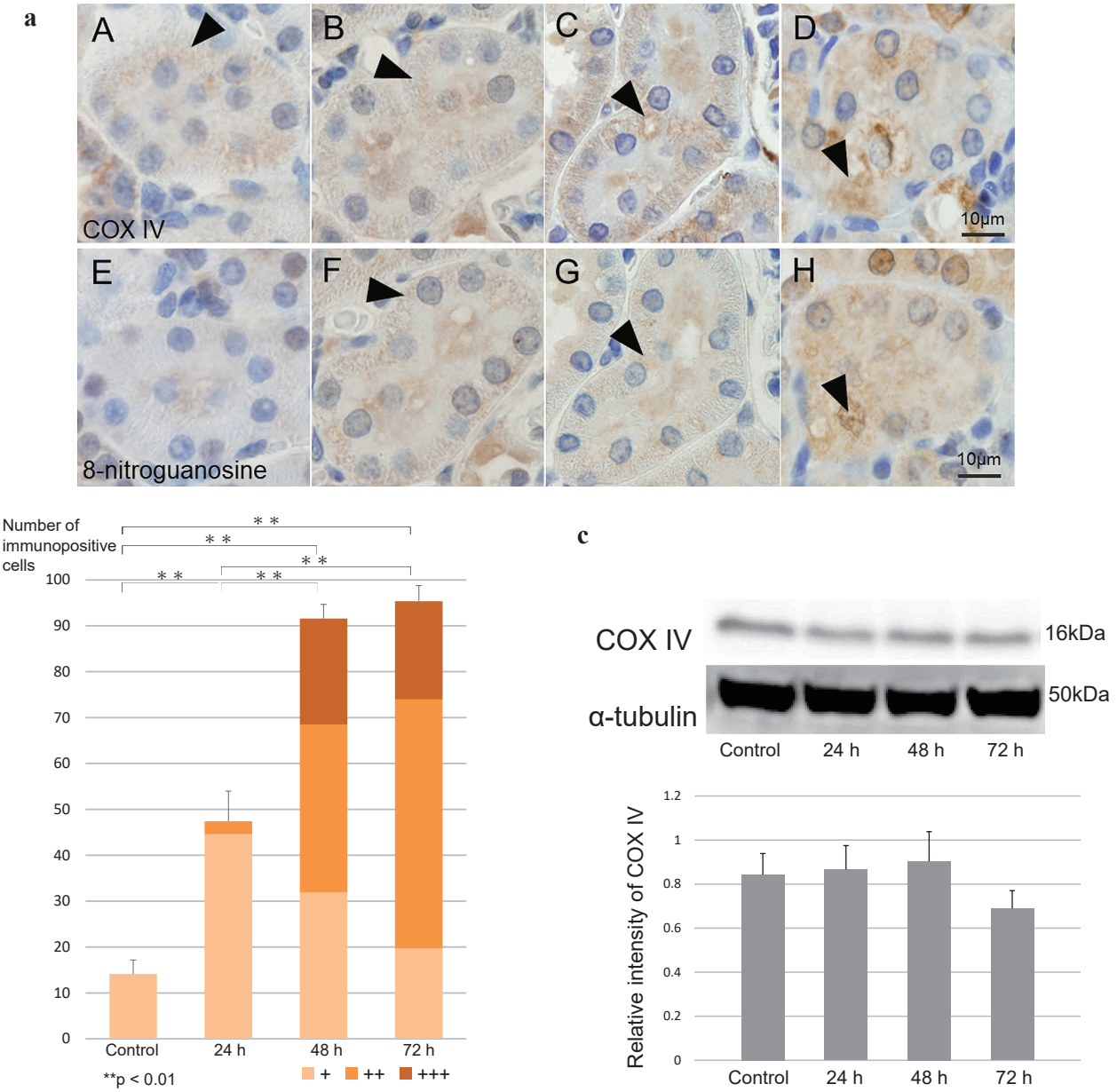

Fig. 4. COX IV and 8-nitroguanosine positivity in the kidney tissues.
a. Immunohistochemistry of COX IV and 8-nitroguanosine in the kidney tissues. Co-localization of the immunopositive granular findings (arrow heads) of COX IV (upper panel) and 8-nitroguanosine (lower panel) is shown in serial section of the kidney tissues. Larger granular appearance of both COX IV and 8-nitroguanosine immunoreactivity is dominated in the degenerated tubules in kidney treated for 72 hours (D, H). A, E, control; B, F, 24 hours after cisplatin treatment; C, G, 48 hours after cisplatin treatment; D, H, 72 hours after cisplatin treatment.
b. Semiquantitative analysis of the immunohistochemical reactions of 8-nitroguanosine in the kidney tissues. Increase in the number of 8-nitroguanosine positive renal epithelial cells is shown in the treated kidneys. h, hour; +, mild positivity; ++, moderate positivity; +++, severe positivity. All data are expressed as mean ± SD. Statistically significant differences (*$p < 0.05$, **$p < 0.01$) are indicated.
c. Expression of COX IV examined by western blotting analysis. Column chart shows relative intensity of COX IV. An increase in COX IV positivity at 24 and 48 hours followed by decrease at 72 hours after treatment is shown in the treated kidney tissues. All data are expressed as mean ± SD. h, hour.

study, a time-dependent increase in both the number of damaged renal tubules and the serum levels of BUN, creatinine, and AST was observed in rats after intraperitoneal administration of cisplatin at 20 mg/kg.

In the past decade, research on cisplatin-mediated nephrotoxicity has gained a significant understanding of the cellular and molecular mechanisms of tubular cell death, revealing the central role of mitochondrial dysregulation in these processes (Ishimoto and Inagi 2016). The pathological degeneration observed in mitochondria, following cispl-

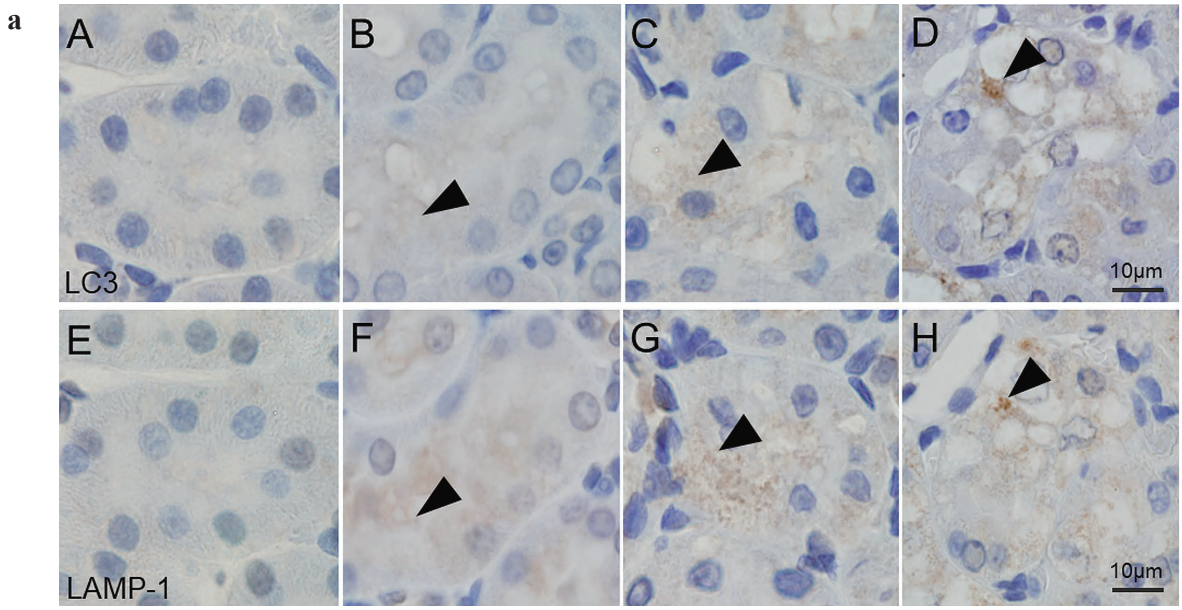

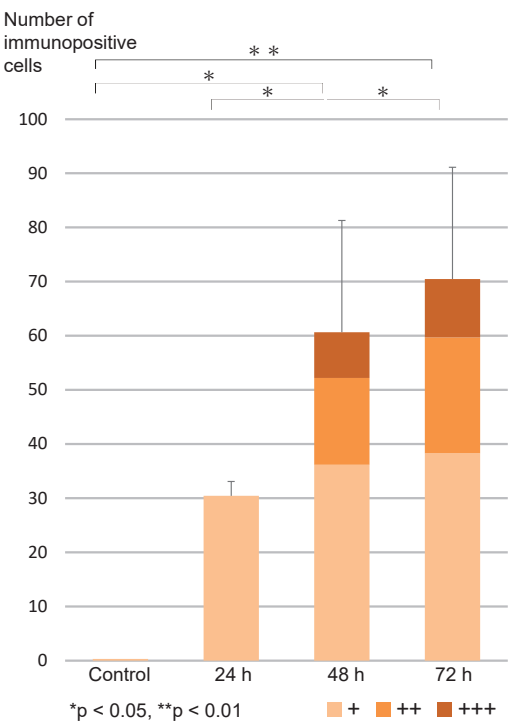

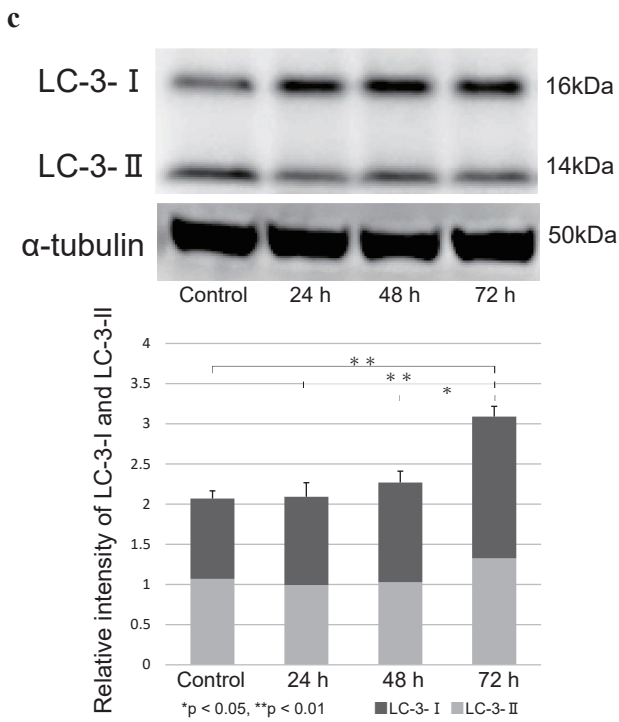

Fig. 5. LC-3 and LAMP-1 positivity in the kidney tissues obtained from cisplatin-treated rats.

a. Immunohistochemistry of LC-3 and LAMP-1 in the kidney tissues. Co-localization of the immunopositive granular findings (arrow heads) of LC-3 (upper panel) and LAMP-1 (lower panel) is shown in serial section of the kidney tissues. Increase in the number of granular findings of both LC-3 and LAMP-1 immunoreactivity is observed in the degenerated tubules (B, F, C, G, D, H). A, E, control; B, F, 24 hours after cisplatin treatment; C, G, 48 hours after cisplatin treatment; D, H, 72 hours after cisplatin treatment.

b. Semiquantitative analysis of the immunohistochemical reactions of LC-3 in the kidney tissues. Increase in the number of LC-3 positive renal epithelial cells is shown in the treated kidneys. h, hour; +, mild positivity; ++, moderate positivity; +++, severe positivity. All data are expressed as mean ± SD. Statistically significant differences (*$p < 0.05$, **$p < 0.01$) are indicated.

c. Expression of LC-3 examined by western blot analysis. Column chart shows relative intensity of LC-3 (LC-3-I and LC-3-II). Increased LC-3 positivity is shown in the treated kidney tissues. All data are expressed as mean ± SD. Statistically significant differences (*$p < 0.05$, **$p < 0.01$) are indicated. h, hour.

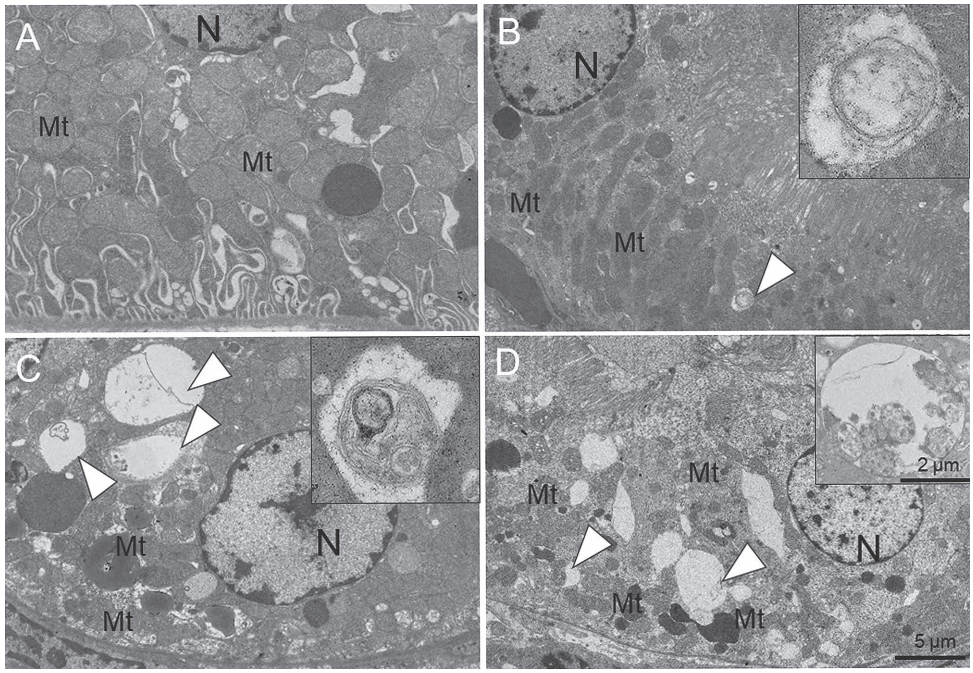

Fig. 6. Electron microscopy of the treated kidney tissues.
Increased number of swollen, dark and fragmented mitochondria (Mt), vacuolar changes (arrow heads) and autophagosomes (inset) containing degenerated mitochondria are shown in the treated kidney tissues (B, C, D).
A, control; B, 24 hours after cisplatin treatment; C, 48 hours after cisplatin treatment; D, 72 hours after cisplatin treatment; N, nucleus; Mt, mitochondria.

atin-mediated nephrotoxicity, is triggered by DNA damage response, pro-apoptotic protein attack, disruption of mitochondrial dynamics, and oxidative stress (Ramesh and Reeves 2002; Pabla and Dong 2008; Mukhopadhyay et al. 2012; Yang et al. 2014). The hypothesis that mitochondrial damage is responsible for cisplatin-induced kidney injury has emerged from studies carried out in cell culture and animal models alike (Gordon and Gattone 1986; Zhang et al. 2006; Mukhopadhyay et al. 2012; Zsengellér et al. 2012; Yang et al. 2014). Pathological features of mitochondrial damage in relation to cisplatin-mediated nephrotoxicity, however, has not been fully described. In this study, both increased numbers of swollen and fragmented mitochondria, observed by electron microscopy, and of COX IV- and 8-nitroguanosine-positive intracytoplasmic granules, detected by immunohistochemistry, were demonstrated in the degenerated renal tubules of the treated animals. An increase in COX IV positivity in western blot analysis at 24 and 48 hours followed by the decrease at 72 hours after treatment indicates mitochondrial hypertrophic reaction at the early stage and resultant loss of mitochondria at the final stage of toxic insult.

AST is an enzyme involved in the transfer of an amino group from aspartate to alpha ketoglutarate to produce oxaloacetic acid and glutamate. More than 80% of AST is localized in the mitochondria while the remaining 20% is localized in the cytoplasm. Cytosolic AST (cAST) promptly appears in the blood from an injured cell. On the contrary, mitochondrial AST (mAST) remains in the core region of an injured cell. Therefore, cumulative activity of mAST in the blood reflects more severe cell damage or necrosis (Kamiike et al. 1989; Chang et al. 2013). In this study, an increased level of mAST was detected in the degenerated renal epithelial cells of rats after intraperitoneal administration of cisplatin at 20 mg/kg, in association with swollen and fragmented mitochondria, observed by electron microscopy, and the presence of COX IV- and 8-nitroguanosine-positive intracytoplasmic granules, detected by immunohistochemistry. These findings suggest that mAST could be one of the serum parameters that can indicate the presence of mitochondrial-targeted cellular toxicity.

A previous study has shown that cisplatin treatment of GFP-LC3 (green fluorescent protein-LC3) transgenic mice induced autophagy in kidney proximal tubules in a time-dependent manner (Takahashi et al. 2012). In this study, an increase in LC-3 positivity was detected by western blot analysis and an increase in the number of both LC-3- and LAMP-1-positive granules was observed in the cytoplasm of renal epithelial cells of the renal tissues from the treated animals. In serial sections of the renal tissue, co-localization of LC-3 and LAMP-1 in granules was observed, indicating an activated autophagy process. Electron microscopy helped to identify signs of mitophagy, such as swollen and fragmented mitochondria in autophagosomes, indicating clearance of damaged mitochondria by mitophagy. Necrosis of the tubular epithelial cells would be visible when the accumulation of damaged mitochondria outpaces the clearance by mitophagy. Removal of damaged

mitochondria, which could be the source of ROS that is harmful to the cellular components, by induction of mitophagy is now one of the therapeutic targets to block drug-induced nephrotoxicity (Takahashi et al. 2012; Tang et al. 2015; Cui et al. 2015; Zhao et al. 2107a, b).

Acknowledgments

We would like to thank Editage (https://www.editage.jp) for English language editing.

Conflict of Interest

The authors declare no conflict of interest.

References

Chang, W.J., Joe, K.T., Park, H.Y., Jeong, J.D. & Lee, D.H. (2013) The relationship of liver function tests to mixed exposure to lead and organic solvents. *Ann. Occup. Environ. Med.*, **25**, 5.

Choi, Y.M., Kim, H.K., Shim, W., Anwar, M.A., Kwon, J.W., Kwon, H.K., Kim, H.J., Jeong, H., Kim, H.M., Hwang, D., Kim, H.S. & Choi, S. (2015) Mechanism of cisplatin-induced cytotoxicity is correlated to impaired metabolism due to mitochondrial ROS generation. *PLoS One*, **10**, e0135083.

Cui, J., Bai, X.Y., Sun, X., Cai, G., Hong, Q., Ding, R. & Chen, X. (2015) Rapamycin protects against gentamicin-induced acute kidney injury via autophagy in mini-pig models. *Sci. Rep.*, **5**, 11256.

Dobyan, D.C., Levi, J., Jacobs, C., Kosek, J. & Weiner, M.W. (1980) Mechanism of cis-platinum nephrotoxicity: II. morphologic observations. *J. Pharmacol. Exp. Ther.*, **213**, 551-556.

Gordon, J.A. & Gattone, V.H. 2nd. (1986) Mitochondrial alterations in cisplatin-induced acute renal failure. *Am. J. Physiol.*, **250**, F991-998.

He, C. & Klionsky, D.J. (2009) Regulation mechanisms and signaling pathways of autophagy. *Annu. Rev. Genet.*, **43**, 67-93.

Ishimoto, Y. & Inagi, R. (2016) Mitochondria: a therapeutic target in acute kidney injury. *Nephrol. Dial. Transplant.*, **31**, 1062-1069.

Kamiike, W., Fujikawa, M., Koseki, M., Sumimura, J., Miyata, M., Kawashima, Y., Wada, H. & Tagawa, K. (1989) Different patterns of leakage of cytosolic and mitochondrial enzymes. *Clin. Chim. Acta*, **185**, 265-270.

Mukhopadhyay, P., Horváth, B., Zsengellér, Z., Zielonka, J., Tanchian, G., Holovac, E., Kechrid, M., Patel, V., Stillman, I.E., Parikh, S.M., Joseph, J., Kalyanaraman, B. & Pacher, P. (2012) Mitochondrial-targeted antioxidants represent a promising approach for prevention of cisplatin-induced nephropathy. *Free Radic. Biol. Med.*, **52**, 497-506.

Pabla, N. & Dong, Z. (2008) Cisplatin nephrotoxicity: mechanisms and renoprotective strategies. *Kidney Int.*, **73**, 994-1007.

Periyasamy-Thandavan, S., Jiang, M., Wei, Q., Smith, R., Yin, X.M. & Dong, Z. (2008) Autophagy is cytoprotective during cisplatin injury of renal proximal tubular cells. *Kidney Int.*, **74**, 631-640.

Ramesh, G. & Reeves, W.B. (2002) TNF-alpha mediates chemokine and cytokine expression and renal injury in cisplatin nephrotoxicity. *J. Clin. Invest.*, **110**, 835-842.

Racusen, L.C. & Solez, K. (1986) Nephrotoxic tubular and interstitial lesions: morphology and classification. *Toxicol. Pathol.*, **14**, 45-57.

Sastry, J. & Kellie, S.J. (2005) Severe neurotoxicity, ototoxicity and nephrotoxicity following high-dose cisplatin and amifostine. *Pediatr. Hematol. Oncol.*, **22**, 441-445.

Tang, C., He, L., Liu, J. & Dong, Z. (2015) Mitophagy: basic mechanism and potential role in kidney diseases. *Kidney Dis* (*Basel*)., **1**, 71-79.

Tsang, R.Y., Al-Fayea, T. & Au, H.J. (2009) Cisplatin overdose: toxicities and management. *Drug Saf.*, **32**, 1109-1122.

Takahashi, A., Kimura, T., Takabatake, Y., Namba, T., Kaimori, J., Kitamura, H., Matsui, I., Niimura, F., Matsusaka, T., Fujita, N., Yoshimori, T., Isaka, Y. & Rakugi, H. (2012) Autophagy guards against cisplatin-induced acute kidney injury. *Am. J. Pathol.*, **180**, 517-525.

Yang, Y., Liu, H., Liu, F. & Dong, Z. (2014) Mitochondrial dysregulation and protection in cisplatin nephrotoxicity. *Arch. Toxicol.*, **88**, 1249-1256.

Zhang, L., Cooper, A.J., Krasnikov, B.F., Xu, H., Bubber, P., Pinto, J.T., Gibson, G.E. & Hanigan, M.H. (2006) Cisplatin-induced toxicity is associated with platinum deposition in mouse kidney mitochondria in vivo and with selective inactivation of the α-ketoglutarate dehydrogenase complex in LLC-PK1 cells. *Biochemistry*, **45**, 8959-8971.

Zhao, C., Chen, Z., Qi, J., Duan, S., Huang, Z., Zhang, C., Wu, L., Zeng, M., Zhang, B., Wang, N., Mao, H., Zhang, A., Xing, C. & Yuan, Y. (2017a) Drp1-dependent mitophagy protects against cisplatin-induced apoptosis of renal tubular epithelial cells by improving mitochondrial function. *Oncotarget*, **8**, 20988-21000.

Zhao, C., Chen, Z., Xu, X., An, X., Duan, S., Huang, Z., Zhang, C., Wu, L., Zhang, B., Zhang, A., Xing, C. & Yuan, Y. (2017b) Pink1/Parkin-mediated mitophagy play a protective role in cisplatin induced renal tubular epithelial cells injury. *Exp. Cell Res.*, **350**, 390-397.

Zsengellér, Z.K., Ellezian, L., Brown, D., Horváth, B., Mukhopadhyay, P., Kalyanaraman, B., Parikh, S.M., Karumanchi, S.A., Stillman, I.E. & Pacher, P. (2012) Cisplatin nephrotoxicity involves mitochondrial injury with impaired tubular mitochondrial enzyme activity. *J. Histochem. Cytochem.*, **60**, 521-529.